JOURNAL OF CATALYSIS 45, 349–355 (1976)

Defect Control of Hydrogenation Activity of Molybdenum Sulfide Catalyst[1]

P. R. WENTRCEK AND H. WISE

Solid State Catalysis Laboratory, Stanford Research Institute, Menlo Park, California 94025

Received June 7, 1976

In line with the observations made in our studies on hydrodesulfurization the defect structure of the molybdenite crystal catalyst controls olefin hydrogenation activity. By exposure of the catalyst to H_2S/H_2 gas mixtures at elevated temperatures the ratio of Mo:S in the catalyst could be adjusted and monitored by electrical conductivity measurements. With a catalyst exhibiting initially *n*-type conductivity the introduction of S^{2-} ions into the solid led to a decrease in electron density and anion vacancies. Further sulfiding of the catalyst led to *p*-type conductivity. The catalytic measurements indicate a pronounced enhancement in olefin hydrogenation activity with the addition of sulfur ions to the solid, i.e., decrease in Mo^{4+}/S^{2-}. The results demonstrate a close relationship between the defect structure of the catalyst and hydrogenation activity.

INTRODUCTION

The hydrogenation of olefins and aromatics catalyzed by metal sulfide catalysts has been reported to occur quite readily for the W–Ni (*1*) and Mo–Co systems (*2*, *3*). In addition, selective hydrogenation of diolefins in olefinic hydrocarbon streams in the presence of presulfided $Co \cdot Mo \cdot Al_2O_3$ has been reported (*4*). For hydrodesulfurization (HDS) of thiophene in the presence of $Co/Mo/Al_2O_3$ catalyst reduction of Mo^{6+} by hydrogen is considered to be an important step in the activation of the catalyst (*5*). These results are not necessarily in conflict with the observations (*6*) that sulfidation of the $Co/Mo/Al_2O_3$ catalyst is essential for HDS catalyst. Rather the data suggest that sulfidation of the catalyst either by pretreatment in H_2S or exposure to a sulfur-bearing compound, such as thiophene, proceeds most readily by way of the Mo^{4+} oxidation state, i.e., Mo^{6+} is first reduced to Mo^{4+} before the sulfide is formed. It is of interest to note that in our studies with a single crystal of MoS_2, the degree of conversion and the product distribution resulting from HDS of butylmercaptan were sensitive functions of the Mo/S ratio of the catalyst as monitored by the electrical conductivity of the crystal catalyst (*7*). At high values of Mo/S, corresponding to the initial stages of sulfidation of the highly reduced catalyst, the conversion of C_4H_9SH was found to be low with the butene isomers as the major products. As the Mo/S ratio decreased and approached the stoichiometric value (Mo/S = 0.5), the conversion of reactant increased markedly and butane prevailed in the product stream. The question arises whether this change in catalytic activity and selectivity is indicative of a mechanism in which the highly sulfided catalyst is capable of hydrogenating the butene formed as a primary product in

[1] This work was sponsored by a group of industrial companies whose support is gratefully acknowledged.

the HDS reaction. Formation of an olefinic species during HDS would be favored in view of the product distribution from HDS of thiophene in the presence of D_2 (*8*).

To examine the olefin hydrogenation activity of MoS_2 we initiated a series of experiments on the hydrogenation of 1-butene as a function of the Mo/S of the crystal catalyst.

EXPERIMENTAL DETAILS

A. Apparatus

The apparatus was identical to that described previously (*7*). It was operated in the pulse mode of a microreactor system in which an aliquot on 1-butene was injected into the carrier system of hydrogen. The sample passed through the reactor containing the MoS_2 catalyst crystal and into the gas chromatograph for chemical analysis. For separation of the various butene isomers from butane a Porasil[2]-packed column was employed, operating at 338 K with hydrogen carrier gas. For *in situ* pretreatment of the catalyst with H_2S/H_2, a special gas line was provided that entered the reactor but bypassed the gas chromatographic system.

The catalyst, in the form of a small single crystal ($1 \times 1 \times 0.086$ cm^3), was cut from a larger crystal of naturally occurring molybdenite[3] (hexagonal crystal structure C7). It was mounted in a quartz reactor provided with Pt feedthroughs for electrical conductivity measurements by the four-probe technique (*7*). The electrical conductors were made of Pt wire (0.0075 cm in thickness) and attached to the four corners of the square crystals.[4] Good electrical contact was achieved by drilling a small hole in each corner of the crystal and tightly looping the Pt wire through the opening and around the crystal. The resistivity of the crystal was measured and found to be 5.5 ohm·cm at 298 K, a value comparable to that reported for molybdenum sulfide (*9*).

B. Method of Defect Control

The degree of nonstoichiometry (Mo/S $\gtrless \frac{1}{2}$) and the type of impurities present in the solid affect the electronic properties of molybdenum sulfide. Thus, the introduction of S^{2-} anions into the MoS_2 lattice tends toward *p*-type conductivity, while sulfur deficiency from the MoS_2 lattice leads to *n*-type behavior. By exposure of the crystal to H_2S/H_2 gas mixtures, i.e., establishment of a specified sulfur vapor pressure at a given temperature, the electronic properties of the crystal may be modified. The layer structure of hexagonal MoS_2 favors rapid transport of ionic species within the lattice and equilibrium of bulk and surface properties at elevated temperatures. Also measurements of electrical conductivity, after establishment of equilibrium at the gas/solid interface, permit identification of the type of lattice defects.

For the *n*-type molybdenum sulfide crystal, the starting material in our studies, the interaction with a sulfur-containing atmosphere may be formulated as

$$S_2 + 4e + 2V_a \rightleftarrows 2S^{2-}, \qquad (1)$$

where e represents an electron and V_a an unoccupied anion vacancy, with an effective charge of +2 relative to the normal lattice since it can trap one or two electrons. Reaction (1) in the forward direction describes the addition of sulfurs to the lattice with depletion of electrons and anion vacancies.

For small concentrations of vacancies, i.e., $S^{2-} \approx$ constant, the law of mass action yields at equilibrium:

$$K = \frac{1}{p_{S_2}[n_e]^4[V_a]^2} \alpha \frac{1}{p_{S_2}[\sigma]^6}, \qquad (2)$$

[2] Porasil, a product of Pechiney-Saint-Gobin, is distributed by Waters Associates, Inc.

[3] This material was kindly provided by Climax Molybdenum Co. of Michigan.

[4] The contribution of these Pt conductors to hydrogenation was found to be negligible, undoubtedly due to their small total surface area and poisoning by sulfur.

where $[n_e]$ denotes the electron density and $[V_a]$ the anion vacancy density. Since the electrons and vacancies contribute to conduction, the electrical conductivity is given by:

$$\sigma\alpha(Kp_{S_2})^{-1/6}, \quad (3)$$

i.e., the conductivity is inversely proportional to the sulfur pressure raised to the $\frac{1}{6}$ power. By analogous reasoning the prevalence of a singly charged lattice defect (V_a^-) would yield a conductivity dependence on sulfur pressure

$$\sigma\alpha(K'p_{S_2})^{-\frac{1}{4}}, \quad (4)$$

and for a doubly charged imperfecton (V_a^{2-})

$$\sigma\alpha(K''p_{S_2})^{-\frac{1}{3}}. \quad (5)$$

Thus, measurement of the electrical conductivity as a function of sulfur pressure allows identification of the type of anion vacancy constituting the lattice defect in the catalyst.

For the equilibrium,

$$MoS_2 \rightleftarrows Mo + S_2, \quad (a)$$

the equilibrium constant is given by

$$K_a = P_{S_2}.$$

It was evaluated from the combination of the following two reactions and their corresponding equilibrium constants:

$$MoS_2 + 2H_2 \rightleftarrows Mo + 2H_2S, \quad (b)$$

$$2H_2S \rightleftarrows 2H_2 + S_2, \quad (c)$$

thus

$$K_a = K_b \cdot K_c.$$

The values for K_b and K_c over a range of temperatures were taken from the literature (*11*). Typical data calculated for the equilibrium (a) are summarized in Table 1.

For reaction (c) the equilibrium partial pressure of sulfur (p_{S_2}) was computed over a range of temperatures and H_2S/H_2 ratios (Table 2). Thus, by adjustment of this ratio and the temperature the desired equilibrium pressures of sulfur could be selected for the controlled conductivity studies with MoS_2.

TABLE 1

Equilibrium calculation for $MoS_2 \rightleftarrows Mo + S_2$

Temp (K)	log K_b	log K_c	log K_a	p_{S_2} (atm)
1073	−2.57	−1.83	−4.40	4.0×10^{-5}
1173	−2.08	−1.45	−3.53	3.0×10^{-4}
1273	−1.92	−1.13	−3.05	8.9×10^{-4}
1373	−1.50	−0.88	−2.38	4.2×10^{-3}

The crystal was equilibrated with the H_2S/H_2 mixture at 893 K and rapidly quenched to room temperature. The electrical conductivity measurements on the sample were carried out in He by the four-probe technique.

EXPERIMENTAL RESULTS

A. *Controlled Conductivity Studies*

The electronic carrier densities of the molybdenite crystal on exposure to H_2S/H_2 gas mixtures of different composition are summarized in Fig. 1 where the electrical conductivity has been plotted as a function of the sulfur pressure in a logarithmic plot. From the slope of the resulting line one calculates a negative conductivity exponent of $\frac{1}{10}$. Although this value is somewhat lower than the theoretical value given by Eq. (3), the data point to the mechanism expressed by reaction (1) as the dominating defect mechanism. Most likely the discrepancy in the conduction coefficient is associated with inadequate quenching of the equilibrium composition and/or the presence of impurities in the crystal with energy levels close to the conduction band.

The anion vacancy V_a may be identified with an unoccupied V_a^- level in the schematic band diagram shown in Fig. 2. Such localized levels located between the valence and conduction band of the semiconductor result from a perturbation of the local potential in the solid by the anion vacancies. It is of interest to note that the V_a^-

TABLE 2

Partial Pressures of Sulfur in Equilibrium with Hydrogen Sulfide–Hydrogen Mixtures

H_2S/H_2	log p_{S_2} (atm)	
	800 K	1000 K
1/3	−7.48	−5.10
1/2	−7.12	−4.64
1/1	−6.52	−4.24
2/1	−5.92	−3.64
3/1	−5.56	−3.29
4/1	−5.32	−3.04
7/1	−4.83	−2.60

level is expected to be close to the impurity level of Co^{2+}, when such a cation is added to the crystal as a doping agent. On this basis it would be expected that the electronic properties of *n*-type molybdenite would be affected in a similar way by the addition of S^{2-} anions or Co^{2+} cations to the lattice of *n*-type MoS_2. This is borne out by the experimental measurements, which demonstrated at $H_2S/H_2 > 5$ a large increase in electrical conductivity with conversion from *n*-type to *p*-type behavior. A similar switch in carrier type results (*10*) from doping *n*-type molybdenite with Co^{2+}.

In the presence of H_2S/H_2 mixtures we estimate such a change from *n*-type to *p*-type conductivity at a room temperature conductivity of 0.5 ohm·cm^{-1} and an equilibrium sulfur pressure of 7×10^{-5} atm. Based on the conductivity measurement, we have constructed the curve in Fig. 3 which demonstrates the variation in electronic properties with defect structure. With the aid of electron mobility data (*1*) for molybdenite the electron carrier densities are estimated to be in the range from 10^{17} to 10^{18} electrons/cm^3 over the range of sulfur pressures examined.

B. Hydrogenation Activity

The hydrogenation activity of the molybdenite catalyst was evaluated at 623 K by injecting pulses of 1-butene into the H_2 carrier stream and monitoring the degree of conversion to butane. The quantity of 1-butene in the pulse was 5×10^{-5} mole and the level of hydrogenation under the experimental conditions ranged up to about 25 vol%. As shown by the data in Fig. 4, a catalyst highly deficient in sulfur, i.e., high electron density, exhibited very low butane formation. With progressive sulfiding of the catalyst a rapid increase in hydrogenation activity was noted.

These results parallel some earlier experiments (*7*) on HDS of butylmercaptan in which the formation of butene was noted as a major product for catalysts with a high Mo/S^{2-} ratio. However, the introduction of S^{2-} ions into the catalyst, by exposure to H_2S/H_2 gas mixtures resulted in the predominance of butane in the product stream. On the basis of the current result it cannot be concluded that butene is an intermediate in the HDS of butylmercaptan.

DISCUSSION

In view of our results, the hydrogenation activity of molybdenum sulfide based catalysts needs to take into account the Mo/S ratio of the catalyst. Russian workers (*12*) varied in a semiquantitative manner the sulfur content in molybdenum sulfide catalysts on activated charcoal and noted

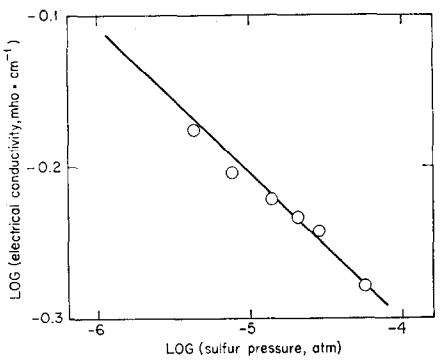

FIG. 1. Variation of electrical conductivity of MoS_2 with sulfur pressure (conductivity measured at 298 K after quenching sample from equilibrium temperature 893 K).

a marked increase in benzene hydrogenation as the ratio of Mo/S was diminished. Our results suggest that this promotion in hydrogenation activity caused by the introduction of S^{2-} ions into the molybdenite crystal is due to changes in the defect structure of the material. The parallelism observed between HDS and hydrogenation activity points to the activated chemisorption of hydrogen as the key step for both processes.

How can the electronic structure of the solid affect the chemisorption process and the type of different adsorbate species present on the catalyst surface during olefin hydrogenation? We choose to interpret our results in terms of an electronic band model involving localized electronic levels at the surface, i.e., surface state energy levels. According to this concept (*13*) the relative surface density of the various adspecies, both charged and uncharged, is governed by the position of the Fermi level E_F of the semiconductor in relation to the surface state energy levels E_t of the adsorbate. Their role in catalytic processes has been examined (*14*) and applied to the oxidation of propylene catalyzed by cuprous oxide (*15*). At equilibrium for a singly charged surface state the ratio of filled n_t to unfilled p_t levels is given by

$$n_t/p_t = \exp[-(E_t - E_F)/kT],$$

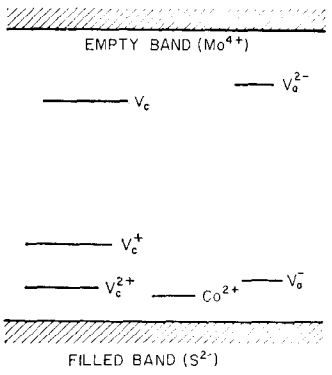

FIG. 2. General band diagram for MoS_2.

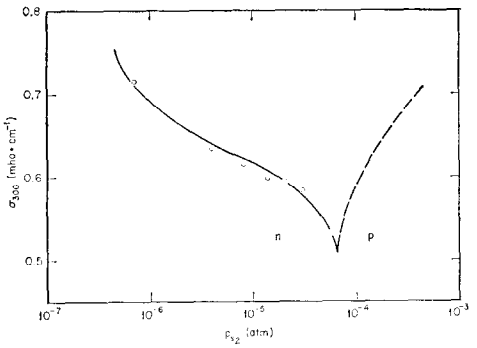

FIG. 3. Electrical conductivity of molybdenite equilibrated with sulfur at 893 K and quenched to 300 K.

where T represents the temperature of the solid. Thus, for $E_t > E_F$ one expects to find few occupied surface states. Instead, electron transfer from a donor-type surface state to the conduction band of the solid is favored, which in the case of hydrogen adspecies leads to the formation of H_s^+ (Fig. 5). The larger the difference $E_t - E_F$ the greater the thermodynamic driving force for electron transfer in that direction. However, the accumulation of positive charges on the surface leads to the establishment of an accumulation space charge layer, i.e., the valence and conduction bands near the surface bend downward relative to the Fermi level (Fig. 5). At the same time the surface state levels in the band gap region change their position in such a way as to maintain a constant energy difference between E_t and E_c. Once the condition is reached that $E_t < E_F$, the thermodynamics of the system favor occupation of the surface state level, i.e., predominance of H adatoms over H^+ adspecies.

It is obvious that the greater the energy difference $E_t - E_F$ the greater the degree of band bending required to attain this reversal in predominance of unoccupied over occupied surface states. The magnitude of the space charge in the surface layer may terminate the process well before the condition $E_t < E_F$ is reached, de-

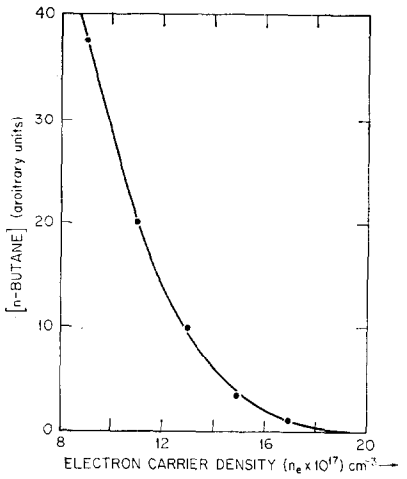

FIG. 4. Catalytic activity of molybdenite for 1-butene hydrogenation at 623 K.

pending on the absolute magnitude of $[E_t - E_F]$. The introduction of S^{2-} ions into the solid leads to lowering of the Fermi level, i.e., makes the molybdenite catalyst less *n*-type, thereby promoting the existence of H^+ adspecies on the surface. Similar defect control can be achieved by doping the crystal with Co^{2+}, thereby making it *p*-type and reducing the Fermi level even further. The difference between these two approaches is one of degree rather than principle, since in each case modification of the Fermi level is the effect desired.

Having established the protonic nature of hydrogen adatoms as the necessary reaction intermediates in the hydrogenation reaction, one may inquire into the mechanism of the olefin conversions. From the observed decrease in electrical conductivity on exposure of the catalyst crystal to butene one may conclude that the olefin molecule adsorbs and occupies an acceptor-type surface state with an energy level below E_F. Thus, occupation of this surface state results in the formation of a negatively charged olefin admolecule ($C_4H_8^-$). On this basis we can postulate a reaction mechanism involving charged surface species:

$$H_2(g) \rightarrow 2\,H(s)$$
$$H(s) \rightleftarrows H^+ + e \qquad (6)$$

$$C_4H_8(g) + e \rightleftarrows C_4H_8^- \qquad (7)$$

$$C_4H_8^- + H^+ \rightleftarrows C_4H_9(s) \qquad (8)$$

$$C_4H_9(s) + H^+ \rightleftarrows C_4H_{10}^+ \qquad (9)$$

$$C_4H_{10}^+ + e \rightleftarrows C_4H_{10}(g) \qquad (10)$$

where all the charged species are on the surface, and the symbols (s) and (g) refer to neutral surface or gas species. Overall, the process depicted in the mechanism results in charge neutrality of the catalyst. The possibility that step (9) involves a neutral H adatom:

$$C_4H_9(s) + H(s) \rightarrow C_4H_{10}(g), \qquad (11)$$

cannot be ruled out.

In line with this mechanism it may be surmised that the intermediate $C_4H_9(s)$ should be able to undergo nonskeletal isomerization. Such catalytic properties have been observed in butadiene (*4*) and butene hydrogenation (*4*, *16*) on sulfide Co–Mo catalysts. Based on our results, the isomerization activity would be expected to be optimized at moderate levels of the Mo/S ratio and low partial pressures of hydrogen. Such conditions would allow formation of the C_4H_9-radical intermediate without further hydrogenation to C_4H_{10}. However, a MoS_2 catalyst with sulfur excess (relative to stoichiometric com-

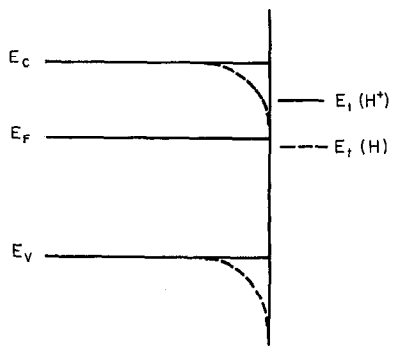

FIG. 5. Surface state energy level diagram.

position) or a Co^{2+}-doped catalyst would favor olefin hydrogenation as observed experimentally.

REFERENCES

1. Voorhoeve, R. J. H., and Stuiver, J. C. M., *J. Catal.* **23**, 228 (1971).
2. Owens, P. J., and Amberg, C. H., *Advan. Chem. Ser.* **33**, 182 (1961).
3. De Beer, V. H. J., Dahlmans, J. G. J., and Smeets, J. G. M., *J. Catal.* **35**, 297 (1974).
4. Kirsch, F. W., and Shull, S. E., *Ind. Eng. Chem. Prod. Res. Develop* **2**, 48 (1963).
5. Lipsch, J. M. J. G., thesis, Technological University, Eindhoven, The Netherlands, 1968.
6. Blue, E. M., and Spurlock B., *Chem. Eng. Progr.* **56**, 54 (1960).
7. Aoshima, A., and Wise, H., *J. Catal.* **34**, 145 (1974).
8. Mikovsky, R. J., Silverstri, A. J., and Heinemann, H., *J. Catal.* **34**, 324 (1974).
9. Fivaz, R., and Mooser, E., *Phys. Rev.* **163**, 743 (1967).
10. Wentrcek, P. R., and Wise, H., unpublished data.
11. Gerasimov, Y. I., Krestovnikov, A. N., and Shakov, A. S., *Chemical Thermodynamics in Non-Ferrous Metallurgy*, Vol. 3, Engl. Transl. Israel Program for Scientific Translation, Jerusalem, 1965.
12. Pavlova, K. A., Panteleeva, B. D., Deryagena, E. N., and Kalechits, I. V., *Kinet. Catal.* (Engl. Transl.) **6**, 427 (1965).
13. Many, A., Goldstein, Y., and Grover, N. B., "Semiconductor Surfaces." North-Holland, Amsterdam, 1965.
14. Morrison, S. R., *Surface Sci.* **10**, 459 (1968); **50**, 329 (1975).
15. Holbrook, L. L., and Wise, H., *J. Catal.* **20**, 367 (1971).
16. De Beer, V. H. J., Van Sint Fiet, T. H. M., Engelen, J. F., Van Haandel, A. C., Wolfs, M. W. J., Amberg, C. H., and Schuit, G. C. A., *J. Catal.* **27**, 357 (1972).